

Article

## Single-Site Cobalt Catalysts at New Zr( $\mu$ -O)( $\mu$ -OH)( $\mu$ -OH) Metal-Organic Framework Nodes for Highly Active Hydrogenation of Nitroarenes, Nitriles, and Isocyanides

Pengfei Ji, Kuntal Manna, Zekai Lin, Xuanyu Feng, Ania Urban, Yang Song, and Wenbin Lin

*J. Am. Chem. Soc.*, **Just Accepted Manuscript** • Publication Date (Web): 06 May 2017

Downloaded from <http://pubs.acs.org> on May 6, 2017

### Just Accepted

“Just Accepted” manuscripts have been peer-reviewed and accepted for publication. They are posted online prior to technical editing, formatting for publication and author proofing. The American Chemical Society provides “Just Accepted” as a free service to the research community to expedite the dissemination of scientific material as soon as possible after acceptance. “Just Accepted” manuscripts appear in full in PDF format accompanied by an HTML abstract. “Just Accepted” manuscripts have been fully peer reviewed, but should not be considered the official version of record. They are accessible to all readers and citable by the Digital Object Identifier (DOI®). “Just Accepted” is an optional service offered to authors. Therefore, the “Just Accepted” Web site may not include all articles that will be published in the journal. After a manuscript is technically edited and formatted, it will be removed from the “Just Accepted” Web site and published as an ASAP article. Note that technical editing may introduce minor changes to the manuscript text and/or graphics which could affect content, and all legal disclaimers and ethical guidelines that apply to the journal pertain. ACS cannot be held responsible for errors or consequences arising from the use of information contained in these “Just Accepted” manuscripts.



# Single-Site Cobalt Catalysts at New $Zr_{12}(\mu_3-O)_8(\mu_3-OH)_8(\mu_2-OH)_6$ Metal-Organic Framework Nodes for Highly Active Hydrogenation of Nitroarenes, Nitriles, and Isocyanides

Pengfei Ji,<sup>†</sup> Kuntal Manna,<sup>†</sup> Zekai Lin, Xuanyu Feng, Ania Urban, Yang Song, and Wenbin Lin\*

Department of Chemistry, University of Chicago, 929 E 57<sup>th</sup> St, Chicago, IL 60637, USA

**ABSTRACT:** We report here the synthesis of a robust and porous metal-organic framework (MOF),  $Zr_{12}$ -TPDC, constructed from triphenyldicarboxylic acid ( $H_2$ TPDC) and an unprecedented  $Zr_{12}$  secondary building unit (SBU):  $Zr_{12}(\mu_3-O)_8(\mu_3-OH)_8(\mu_2-OH)_6$ . The  $Zr_{12}$  SBU can be viewed as an inorganic node dimerized from two commonly observed  $Zr_6$  clusters via six  $\mu_2$ -OH groups. The metalation of  $Zr_{12}$ -TPDC SBUs with  $CoCl_2$  followed by treatment with  $NaBEt_3H$  afforded a highly active and reusable solid  $Zr_{12}$ -TPDC-Co catalyst for the hydrogenation of nitroarenes, nitriles, and isocyanides to corresponding amines in excellent activity and selectivity. This work highlights the opportunity in designing novel MOF-supported single-site solid catalysts by tuning the electronic and steric properties of the SBUs.

## Introduction

Metal-organic frameworks have become an important class of molecular materials with broad applications in catalysis,<sup>1-8</sup> biomedical imaging and drug delivery,<sup>9-11</sup> gas storage and separation,<sup>12-20</sup> sensing,<sup>21-23</sup> solar energy harvesting,<sup>24-25</sup> and electron and ion conductivity.<sup>26-27</sup> A large diversity of inorganic nodes have been used for MOF construction, including the nodes based on divalent, trivalent, and most importantly, tetravalent metals.<sup>28-29</sup> Among tens of thousands of MOFs synthesized to date,<sup>30-32</sup> Zr-based MOFs have distinguished themselves with exceptionally high thermal and chemical stability, simple and straightforward linker tunability, and relatively low costs of zirconium precursors.<sup>33-34</sup> Depending on choice of linkers and synthetic conditions, several kinds of Zr nodes with different symmetry and connectivity have been obtained, including  $ZrO_6$ ,<sup>35-36</sup>  $Zr_6O_4(\mu_3-OH)_4$ ,<sup>37-38</sup> and  $Zr_8O_8(\mu_2-OH)_4$  nodes.<sup>39-40</sup> Herein we report a new  $Zr_{12}$ -TPDC ( $H_2$ TPDC is triphenyldicarboxylic acid) MOF based on the first example of  $Zr_{12}O_8(\mu_3-OH)_8(\mu_2-OH)_6$  node,<sup>41</sup> and its application in supporting single-site cobalt-based solid catalysts for highly effective hydrogenation of nitroarenes, nitriles, and isocyanides to afford corresponding amines.

We recently showed that the SBUs in Zr MOFs provided an excellent ligand platform for discovering single-site base metal (e.g., Fe and Co) catalysts without homogenous analogs.<sup>39, 42</sup> The bridging ligands of Zr MOFs created a unique bowl-shaped secondary environments around the SBU-supported base metal centers that cannot be easily enforced in homogeneous molecular catalyst systems. More importantly, we discovered that the activities and selectivities of supported base metal catalysts were exquisitely sensitive to subtle steric and electronic differences of Zr SBUs (Figure 1). For example, the  $Zr_6O_4(\mu_3-OCOH)_4$  catalyst based on the  $Zr_6O_4(\mu_3-OH)_4$  node is highly active for benzylic C-H functionalization,<sup>42</sup> while the  $Zr_8O_8(\mu_2-$

$OCOH)_4$  catalyst based on the  $Zr_8O_8(\mu_2-OH)_4$  node effectively hydrogenates hindered alkenes, imines, and heterocycles to afford important fine chemicals.<sup>39</sup>

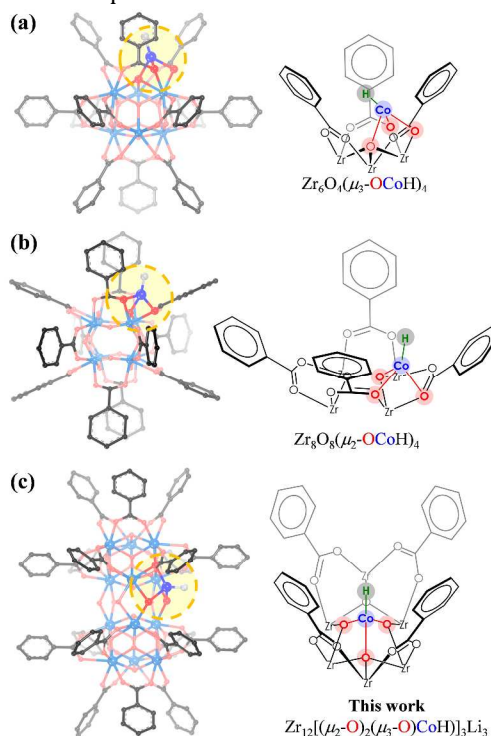


**Figure 1.** Depiction of three Co catalysts with vastly different activities and selectivities based on different SBUs of Zr MOFs. The  $Zr_6O_4(\mu_3-OCOH)_4$  (a),  $Zr_8O_8(\mu_2-OCOH)_4$  (b), and  $Zr_{12}[(\mu_2-O)_2(\mu_3-O)CoH]_3Li_3$  (c) catalysts are generated from the  $Zr_6O_4(\mu_3-OH)_4$ ,  $Zr_8O_8(\mu_2-OH)_4$ , and  $Zr_{12}O_8(\mu_3-OH)_8(\mu_2-OH)_6$  nodes, respectively.

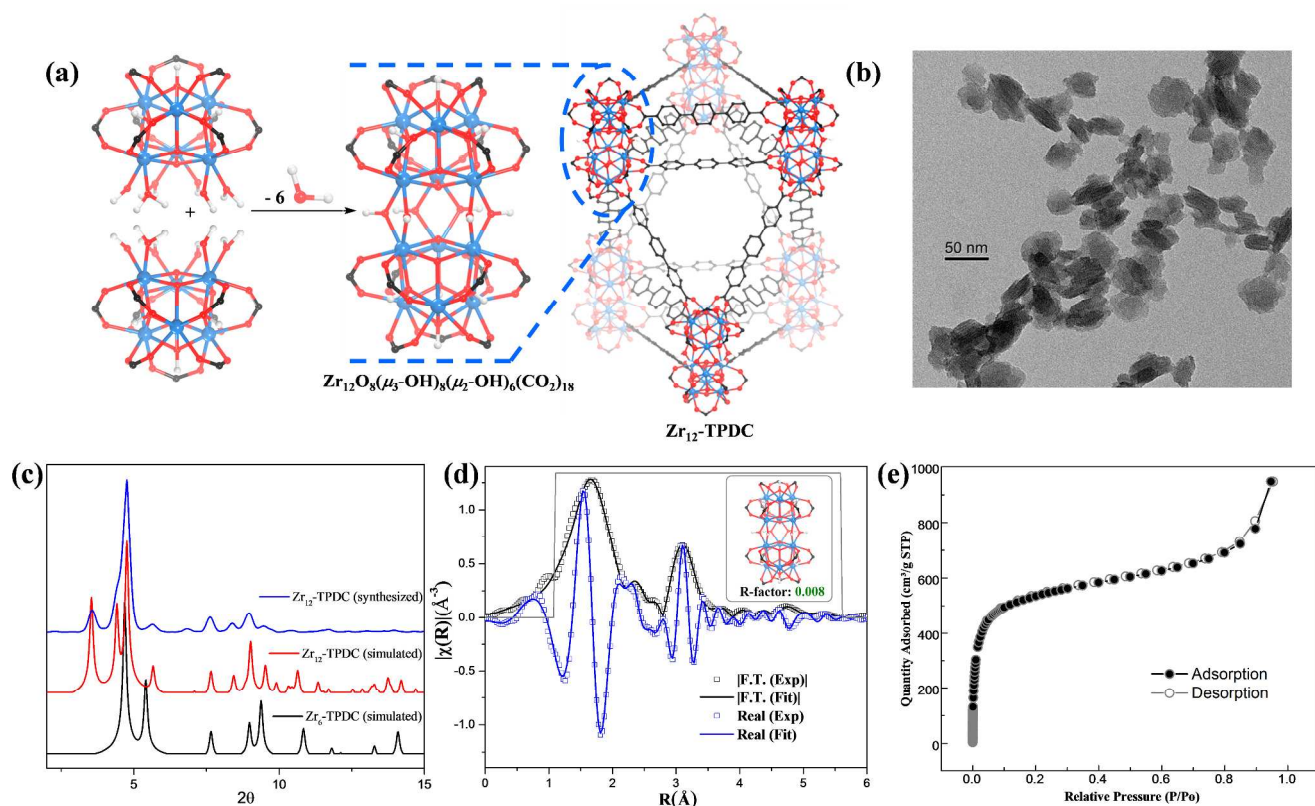


**Figure 2.** (a) The SBU of  $Zr_{12}$ -TPDC formally results from dehydrative condensation of two  $Zr_6$  nodes. (b) TEM image of  $Zr_{12}$ -TPDC showing plate-like morphology. (c) The experimental PXRD pattern of  $Zr_{12}$ -TPDC (blue) is similar to the simulated PXRD of  $Zr_{12}$ -TPDC (red), but very different from the simulated PXRD of  $Zr_6$ -TPDC (black). (d) EXAFS spectra and fits in R-space at the Zr K-edge of  $Zr_{12}$ -TPDC showing the magnitude (hollow squares, black) and real component (hollow squares, blue) of the Fourier transform. The fitting range is 1.1–5.6 Å in R space (within the grey lines). (e) Nitrogen sorption isotherms of  $Zr_{12}$ -TPDC (77 K).

These studies demonstrated the ability to create highly active and selective supported molecular catalysts using Zr nodes in MOFs and inspired our interest in discovering new Zr nodes to support base metal catalysts for other challenging organic transformations. Based on the existence of molecular  $Zr_{12}O_8(\mu_3-OH)_8(\mu_2-OH)_6(RCO_2)_{18}$  ( $R = H$  or  $tBu$ , Figure S1, SI) clusters,<sup>41</sup> we sought to modify the synthetic conditions of UiO-68 in order to obtain a new MOF with the  $Zr_{12}O_8(\mu_3-OH)_8(\mu_2-OH)_6$  node. Gratifyingly, by adding a suitable amount of water to the reaction mixture, we obtained a new  $Zr_{12}$ -TPDC MOF of the formula  $Zr_{12}O_8(\mu_3-OH)_8(\mu_2-OH)_6(TPDC)_9$ .  $Zr_{12}$ -TPDC presumably forms through dimerizing two  $Zr_6$  clusters via six  $\mu_2$ -OH groups as a result of the reduced  $H_2$ TPDC concentration by adding water (Figure 2a).  $Zr_{12}$ -TPDC was postsynthetically metalated with  $CoCl_2$  followed by treatment with  $NaBEt_3H$  to afford a highly active and reusable solid  $Zr_{12}$ -TPDC-Co catalyst for the hydrogenation of nitroarenes, nitriles, and isocyanides to corresponding amines in excellent activity and selectivity.

## Results and Discussion

**Synthesis and Characterization of  $Zr_{12}$ -TPDC.**  $Zr_{12}$ -TPDC was synthesized via a solvothermal reaction between  $ZrCl_4$  and  $H_2$ TPDC in DMF and water at 90 °C using acetic acid as modulator. The resulting white suspension was centrifuged, and then washed with DMF and THF to afford  $Zr_{12}$ -TPDC in 45% yield. Transmission electron microscopy (TEM) showed a disk-like morphology of approximately 40 nm in diameter and 10 nm in thickness (Figure 2b). The

small particle size is advantageous for MOF catalysts due to shorter diffusion distances for both reaction substrates and products, which increases reaction rates.

Atomic structure of the MOF was simulated based on a combination of the crystal structures of the  $Zr_{12}O_8(OH)_8(OH)_6(tBuCO_2)_{18}$  cluster<sup>41</sup> and UiO-68 ( $Zr_6$ -TPDC).<sup>42</sup> The MOF adopts the trigonal  $P\bar{3}1c$  space group, with each  $Zr_{12}$  node coordinating to 18 bridging organic linkers. This structural assignment was supported by the similarity between the simulated powder X-ray diffraction pattern (PXRD) and the experimental PXRD (Figure 2c). The  $2\theta$  peak at  $3.56^\circ$  corresponds to the (002) diffraction with a d spacing of 2.49 nm, which is characteristic of  $Zr_{12}$ -TPDC and results from diffraction between neighboring  $Zr_{12}$  SBUs along the  $c$  axis. This d spacing is larger than the SBU distance of  $Zr_6$ -TPDC (1.88 nm) along the [111] direction. The d spacing of 2.49 nm between  $Zr_{12}$  SBUs is also evidenced in high resolution TEM images of  $Zr_{12}$ -TPDC (Figure S3, SI).

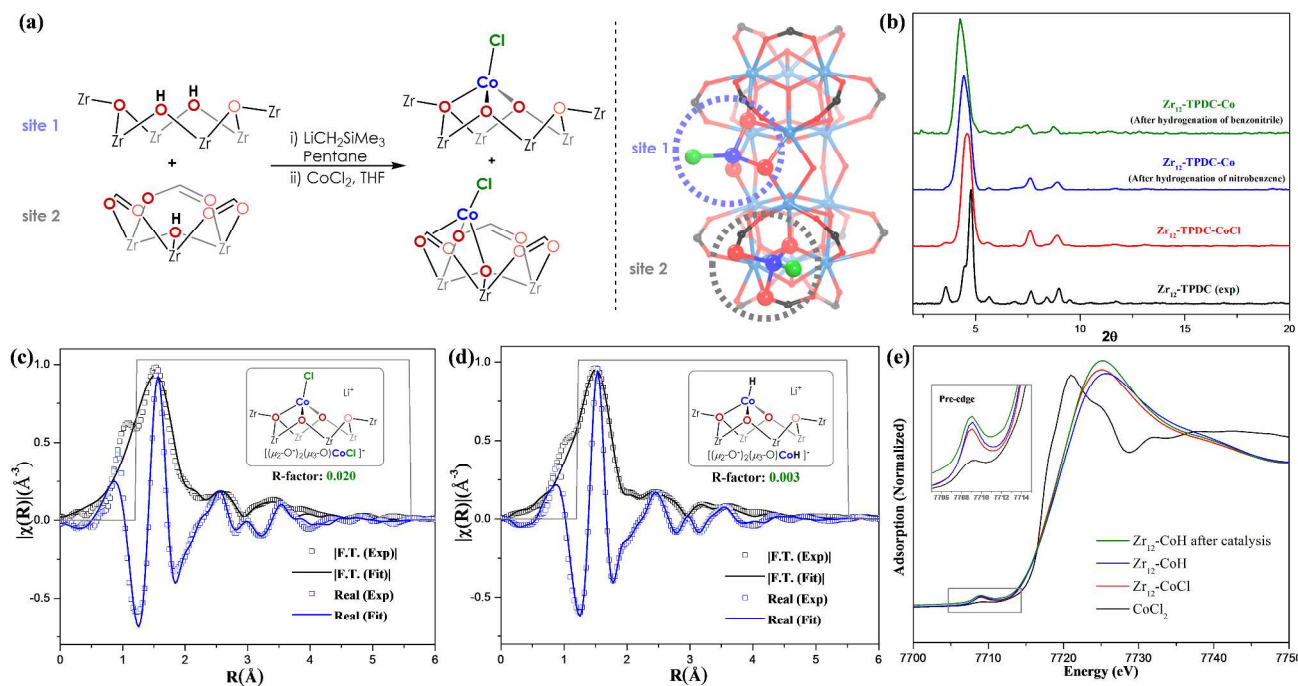


**Figure 3.** (a) The metalation of Zr<sub>12</sub>-SBU with CoCl<sub>2</sub> to form Zr<sub>12</sub>-TPDC-CoCl. (b) Similarities among the PXRD patterns of Zr<sub>12</sub>-TPDC (black) and the PXRD patterns of Zr<sub>12</sub>-TPDC-CoCl (red), Zr<sub>12</sub>-TPDC-Co samples recovered from hydrogenation of nitrobenzene (blue) and benzonitrile (green) show the retention of Zr<sub>12</sub>-TPDC crystallinity after metalation and catalysis. (c) EXAFS spectra and fits in R-space at the Co K-edge of Zr<sub>12</sub>-TPDC-CoCl showing the magnitude (hollow squares, black) and real component (hollow squares, blue) of the Fourier transformation. The fitting range is 1.2 - 5.6 Å in R space (within the grey lines). (d) EXAFS spectra and fits in R-space at the Co K-edge of Zr<sub>12</sub>-TPDC-CoH showing the magnitude (hollow squares, black) and real component (hollow squares, blue) of the Fourier transformation. The fitting range is 1.2 - 5.5 Å in R space (within the grey lines). (e) XANES spectra of Zr<sub>12</sub>-TPDC-CoCl, Zr<sub>12</sub>-TPDC-CoH and Zr<sub>12</sub>-TPDC-Co after nitrobenzene hydrogenation are similar to that of CoCl<sub>2</sub>, indicating a +2 oxidation state of the Co centers in all of the species.

The Zr coordination environment in the Zr<sub>12</sub> SBU was also studied by extended X-ray fine structure (EXAFS) spectroscopy. A good fit with an R-factor of 0.008 was obtained based on the Zr<sub>12</sub> cluster crystal structure (Figure 2d). Thermogravimetric analysis (TGA) showed a weight loss of 65.5% from 240 °C to 800 °C, corresponding well to the decomposition of Zr<sub>12</sub>O<sub>8</sub>(μ<sub>3</sub>-OH)<sub>8</sub>(μ<sub>2</sub>-OH)<sub>6</sub>(TPDC)<sub>9</sub> to (ZrO<sub>2</sub>)<sub>12</sub> (65.7% expected). The observed weight loss is much smaller than that of Zr<sub>6</sub>-TPDC (71.3%) due to the increased Zr weight percentage in Zr<sub>12</sub>-TPDC. N<sub>2</sub> adsorption isotherm of Zr<sub>12</sub>-TPDC showed a type I adsorption (77K, 1 bar) with Brunauer-Emmett-Teller (BET) surface area of 1967 m<sup>2</sup>/g (Figure 2e). The surface area of Zr<sub>12</sub>-TPDC is smaller than that of Zr<sub>6</sub>-TPDC (2815 m<sup>2</sup>/g) due to the increased molecular weight of SBUs and similar pore shape and size.

**Metalation of Zr<sub>12</sub>-TPDC with CoCl<sub>2</sub>.** Zr<sub>12</sub>-TPDC was treated with 5 equiv. of LiCH<sub>2</sub>SiMe<sub>3</sub> to deprotonate both the μ<sub>2</sub>-OH and μ<sub>3</sub>-OH sites in Zr<sub>12</sub> SBU, then reacted with a CoCl<sub>2</sub> solution in THF to afford Zr<sub>12</sub>-TPDC-CoCl as a deep-blue solid (Figure 3a). Crystallinity of the MOF was maintained after metalation, as indicated by the similarity between the PXRD patterns of Zr<sub>12</sub>-TPDC and Zr<sub>12</sub>-TPDC-CoCl (Figure 3b). Inductively coupled plasma-mass spectrometry (ICP-MS) analysis of the digested MOF revealed the presence of 11.2±0.6 Co per Zr<sub>12</sub> cluster, corresponding to complete metalation of all eight μ<sub>3</sub>-OLi sites to form eight (Zr<sub>3</sub>O)CoCl, and all six μ<sub>2</sub>-OLi sites to form three [(Zr<sub>2</sub>O

)<sub>2</sub>(Zr<sub>3</sub>O)CoCl]Li, to give the complete formula of Zr<sub>12</sub>(μ<sub>3</sub>-O)<sub>5</sub>[(μ<sub>3</sub>-O)CoCl]<sub>8</sub>[(μ<sub>2</sub>-O)<sub>2</sub>(μ<sub>3</sub>-O)CoCl]<sub>3</sub>Li<sub>3</sub>(TPDC)<sub>9</sub>.

The coordination environments of the Co centers in Zr<sub>12</sub>-TPDC-CoCl were studied by EXAFS at the Co Kα edge. The six μ<sub>2</sub>-OH sites are very close to each other, with a distance of 3.13 Å between two neighboring sites. From our previous experience with Zr-O-Co systems and reported Co-oxide ligand binding modes, we envisioned three different Co coordination modes on the μ<sub>2</sub>-OH sites: [(μ<sub>2</sub>-O)<sub>2</sub>(μ<sub>3</sub>-O)CoCl]<sup>-</sup> (Figure 3c), [(μ<sub>2</sub>-O)<sub>2</sub>CoCl]<sub>2</sub><sup>2-</sup> (Figure S9, SI) and (μ<sub>2</sub>-O)(μ<sub>3</sub>-O)(μ-CO<sub>2</sub>)CoCl (Figure S10, SI). The [(μ<sub>2</sub>-O)<sub>2</sub>(μ<sub>3</sub>-O)CoCl]<sup>-</sup> model gives the best fit, with a R-factor of 0.020, and the Co-(μ<sub>2</sub>-O) distance of 1.90 Å (Figure 3c). EXAFS fitting with the [(μ<sub>2</sub>-O)<sub>2</sub>CoCl]<sub>2</sub><sup>2-</sup> and (μ<sub>2</sub>-O)(μ<sub>3</sub>-O)(μ-CO<sub>2</sub>)CoCl structure models gave larger R-factors of 0.023 and 0.027, respectively, as a result of misfits in the second shells (R = 2.2-3.2 Å) which is mainly due to the Co contribution to the Zr scattering pathway. The Co centers on the μ<sub>3</sub>-OH sites adopt a (μ<sub>3</sub>-O)(μ-CO<sub>2</sub>)CoCl mode, similar to the structures proposed in previous systems.<sup>42</sup> We further propose the exchange between the μ<sub>3</sub>-O and μ<sub>3</sub>-OLi sites in Zr<sub>12</sub> SBUs after lithiation in order to avoid the steric clash between the μ<sub>3</sub>-OCoCl and [(μ<sub>2</sub>-O)<sub>2</sub>(μ<sub>3</sub>-O)CoCl]<sup>-</sup> moieties that are installed on the adjacent Zr<sub>3</sub>(μ<sub>3</sub>-OH) and (μ<sub>2</sub>-OH)<sub>2</sub> binding sites (Figure 3a and Figure S12, SI).

TGA of the Zr<sub>12</sub>-TPDC-CoCl showed a weight loss of 55.3% from 180 °C to 800 °C (Figure S13, SI), corresponding well to the decomposition of Zr<sub>12</sub>O<sub>5</sub>(OCoCl)<sub>8</sub>(O<sub>3</sub>CoCl)<sub>3</sub>Li<sub>3</sub>(TPDC)<sub>9</sub> to (ZrO<sub>2</sub>)<sub>12</sub>(CoO<sub>1.5</sub>)<sub>11</sub>(LiO<sub>0.5</sub>)<sub>3</sub> (54.5% expected). N<sub>2</sub> sorption

studies indicated that Zr<sub>12</sub>-TPDC-CoCl had a BET surface area of 810 m<sup>2</sup>/g. In contrast to Zr<sub>12</sub>-TPDC which exhibits a Type I adsorption isotherm, Zr<sub>12</sub>-TPDC-CoCl adopts a type II adsorption isotherm (Figure S14, SI), likely due to several distortion of the Zr<sub>12</sub>-TPDC-CoCl framework upon desolvation. The severe framework distortion was also indicated by the loss of PXRD pattern for the dried Zr<sub>12</sub>-TPDC-CoCl sample.

### Zr<sub>12</sub>-TPDC-Co-Catalyzed Hydrogenation of Nitroarenes.

Treatment of Zr<sub>12</sub>-TPDC-CoCl with 5 equiv. of NaBEt<sub>3</sub>H in THF generated the corresponding cobalt-hydride species Zr<sub>12</sub>-TPDC-CoH as a black solid. XANES analysis of Zr<sub>12</sub>-TPDC-CoH suggested +2 oxidation state of the Co centers (Figure 3e). EXAFS study on Zr<sub>12</sub>-TPDC-CoH showed that the [(μ<sub>2</sub>-O)<sub>2</sub>(μ<sub>3</sub>-O)CoH]<sup>-</sup> structural model fit the experimental spectra well, with a R-factor of 0.003. EXAFS fitting also gave a Co-(μ<sub>2</sub>-O) distance of 1.97 Å (Figure 3d).

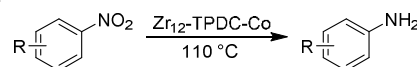
Zr<sub>12</sub>-TPDC-CoH was an active catalyst for hydrogenation of a broad range of nitroarenes to corresponding anilines. Anilines are important building blocks for the synthesis of pharmaceuticals, fine chemicals, and commodities.<sup>43-44</sup> Among the various known procedures for the reduction of nitroarenes, the catalytic hydrogenation represents one of the most efficient and environmentally benign synthetic routes. To date, active and chemoselective catalysts for nitroarene hydrogenation are mostly based on precious and toxic noble metals,<sup>45-47</sup> with a few earth-abundant metal based catalysts recently appeared in the literature.<sup>48-51</sup> The screening experiments for Zr<sub>12</sub>-TPDC-CoH catalyzed hydrogenation revealed that the highest turnover frequencies (TOFs) were obtained when the reactions were performed in toluene at 110 °C. At a 0.5 mol % Co loading, nitrobenzene was completely hydrogenated in toluene at 110 °C under 40 bar of H<sub>2</sub> in 42 h to afford aniline in quantitative yield. Under these reaction conditions, nitroarenes containing oxo- or halogen-functionalities, 4-nitroanisole, 1-nitronaphthalene, 4-nitrobenzotrifluoride, 1-bromo-2-nitrobenzene, 1-bromo-4-nitrobenzene and 1-iodo-4-nitrobenzene, were selectively hydrogenated to afford 4-aminoanisole, 1-naphthylamine, 4-(trifluoromethyl)aniline, 2-bromoaniline, 4-bromoaniline, and 4-iodoaniline, respectively, in 70-100% yields (entries 1-6, Table 1). Pure aniline products were obtained by simple filtration of the reaction mixtures followed by removal of the volatiles (Figure S18, SI). Both electron-poor substituents, such as trifluoromethyl, and electron-rich groups, such as methoxy and amino, were well tolerated under the reaction conditions. The hydrogenation of N-methyl-4-nitroaniline and N,N'-dimethyl-4-nitroaniline afforded 4-(dimethylamino)aniline and 4-(dimethylamino)aniline in excellent yields, respectively (entries 7-8, Table 1).

Impressively, Zr<sub>12</sub>-TPDC-CoH also selectively reduced nitro groups in presence of sensitive substituents such as iodo or keto groups. For example, at a 0.5 - 2.0 mol % Co loading, 1-iodo-4-nitrobenzene, 4-nitrobenzophenone, and 4-nitroacetophenone were selectively hydrogenated to 4-iodoaniline, 4-aminobenzophenone, and 4-aminoacetophenone, respectively, in moderate yields (entries 9-11, Table 1). As heteroaromatic amines are im-

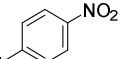
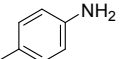
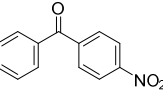
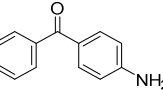
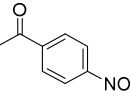
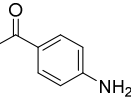
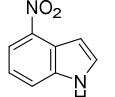
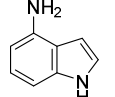
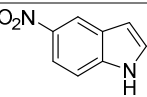
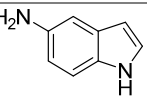
portant building blocks in synthesizing a variety of pharmaceuticals and biologically active compounds, we also tested the hydrogenation of nitroindole compounds. Without any optimization, 4-nitroindole and 5-nitroindole were hydrogenated to afford 4-aminoindole and 5-aminoindole in 55% and 92% isolated yields, respectively, and no by-products were detected in the reaction mixtures (entries 7-8, Table 1).

Importantly, at a 1.0 mol% Co-loading, Zr<sub>12</sub>-TPDC-CoH could be recovered and reused at least 7 times for the hydrogenation of 4-nitroanisole without loss of catalytic activity (Figure 4). Excellent yields (86-100%) of 4-aminoanisole were obtained consistently in the reuse experiments without formation of any by-product (Figure S21, SI). The PXRD pattern of Zr<sub>12</sub>-TPDC-CoH recovered from the first run remained unchanged from that of pristine Zr<sub>12</sub>-TPDC-CoH (Figure 3b), indicating the stability of the MOF structure under the reaction conditions. The heterogeneity of Zr<sub>12</sub>-TPDC-CoH was confirmed by several experiments. ICP-MS analyses showed that the amounts of Co and Zr that leached into the supernatant after the first run were only 0.4% and 0.03%, respectively. Moreover, no additional hydrogenation was observed after removal of the solid catalyst from the reaction mixture. The rate of hydrogenation was unchanged in the presence of metallic mercury. These tests rule out the role of any leached Co-nanoparticles or other Co-species in catalyzing hydrogenation reactions (Figure S20, SI).

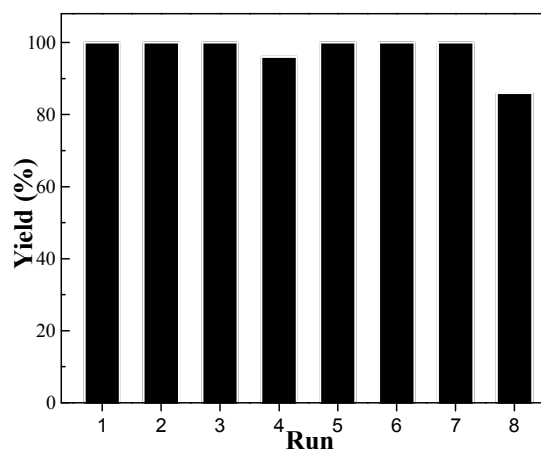
**Table 1.** Zr<sub>12</sub>-TPDC-Co Catalyzed Hydrogenation of Nitroarenes.<sup>a</sup>



Entry	Substrate	Product	Mol % Co	Yield % <sup>b</sup>
1			0.5	100
2			0.5	100 (100)
3			0.5	100 (96)
4			0.5	100 (89)
5			0.5	70
6			0.5	98
7			0.5	47
8			1.0	100

9			0.5	41
10			2.0	72
11			2.0	54
12 <sup>c</sup>			1.0	55
13			2.0	92

<sup>a</sup>Reaction conditions: 0.50 mg of Zr<sub>12</sub>-TPDC-CoCl, 5 equiv of NaBEt<sub>3</sub>H (1.0 M in toluene) w.r.t. Co, nitroarene, toluene, 40 bar H<sub>2</sub>, 110 °C, 42 h. <sup>b</sup>Yield was determined by <sup>1</sup>H NMR with mesitylene as the internal standard. Isolated yields are in parentheses. <sup>c</sup>Reaction was performed for 72 h.

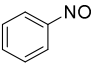
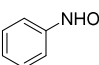
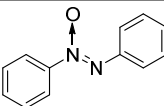
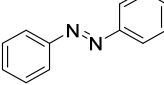
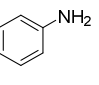
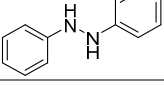
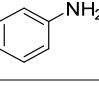


**Figure 4.** Plots of yields (%) of 4-aminoanisole at different runs in the recycle experiments of Zr<sub>12</sub>-TPDC-Co for the hydrogenation of 4-nitroanisole. The Co-loadings were 1.0 mol %.

**Mechanistic Investigation of Zr<sub>12</sub>-TPDC-Co Catalyzed Hydrogenation of Nitroarenes.** To elucidate the multi-step hydrogenation pathways, all possible intermediates in nitrobenzene hydrogenation reactions were tested for reactivity (Table 2). According to literatures,<sup>52</sup> two reaction pathways are possible for nitrobenzene hydrogenation, the monomeric pathway and dimeric pathway. The monomeric pathway reacts by stepwise hydrogenation of nitrobenzene to nitrosobenzene, phenylhydroxyamine, and then aniline. The dimeric pathway is a result of nitrosobenzene reacting with phenylhydroxyamine to form azoxybenzene, which was subsequently hydrogenated to azobenzene, hydrazobenzene, and then aniline. While azobenzene and hydrazobenzene were readily hydrogenated to aniline by Zr<sub>12</sub>-TPDC-Co (Entry 4-5, Table 2), azoxybenzene only gave

7% conversion and 2% yield of aniline under identical reaction conditions, indicating that the azoxybenzene hydrogenation is the slowest step in the dimeric pathway (Entry 5, Table 2). In addition, the rate of hydrogenation of 4-nitroanisole was greatly suppressed in presence of azoxybenzene, indicating that azoxybenzene acts as a catalyst inhibitor (Figure S22, SI). In comparison, hydrogenation of nitrosobenzene and phenylhydroxyamine gave 64-75% yield of aniline together with 22-35% of azoxybenzene side product formed through substrate dimerization (Entry 1-2, Table 2). No azoxybenzene intermediate was observed during hydrogenation of nitrobenzene, presumably because very little nitrosobenzene or phenylhydroxyamine accumulated during the reaction process. With these results, we propose that Zr<sub>12</sub>-TPDC-Co catalyzed nitroarene hydrogenation mainly via the monomeric pathway as shown inside the dotted box in Figure 5.

**Table 2.** Zr<sub>12</sub>-TPDC-Co-Catalyzed Hydrogenation of Intermediates in Proposed Pathways of Nitroarene Hydrogenation.<sup>a</sup>

Entry	Substrate	Product	Conversion % <sup>b</sup>
1		PhN(O)=NPh + PhN=NPh + PhNH <sub>2</sub>	100 (35:1:64)
2		PhN(O)=NPh + PhN=NPh + PhNH <sub>2</sub>	100 (22:3:75)
3		PhN=NPh + PhNH <sub>2</sub>	7 (5:2)
4			100
5			100

<sup>a</sup>Reaction conditions: 0.50 mg of Zr<sub>12</sub>-TPDC-Co (0.5 mol % Co), substrate, toluene, 40 bar H<sub>2</sub>, 110 °C, 42 h. <sup>b</sup>Conversion was determined by GC-MS analysis.

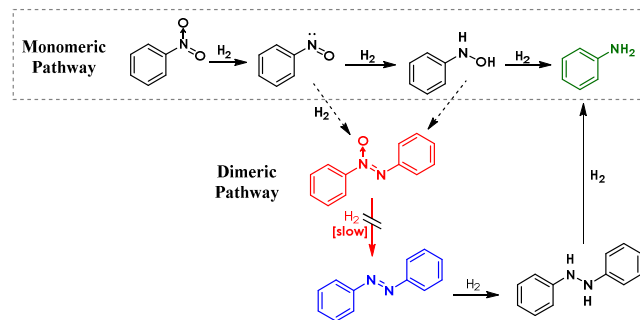


**Figure 5.** Two possible pathways for Zr<sub>12</sub>-TPDC-Co-catalyzed hydrogenation of nitroarenes. Based on our mechanistic studies, we propose that Zr<sub>12</sub>-TPDC-Co catalyzes nitroarene hydrogenation mainly via the monomeric pathway as shown in the dotted box.

**Zr<sub>12</sub>-TPDC-Co-Catalyzed Hydrogenation of Nitriles and Isocyanides.** Zr<sub>12</sub>-TPDC-Co was also active in catalyzing hydrogenation of nitriles and isocyanides. Nitriles are typically reduced to corresponding amines using stoichiometric amounts of metal hydrides,<sup>53</sup> hydrosilanes activated by metals,<sup>54</sup> or organocatalysts.<sup>55</sup> However, these methods have poor atom economy and typically low functional group tolerance. In contrast, catalytic reduction of nitriles using H<sub>2</sub> as the reducing agent is highly atom efficient and sustainable. The single-site hydrogenation catalysts for selective and milder hydrogenation of nitriles have been primarily developed based on precious metals,<sup>56-59</sup> and a few Fe- and Co-based homogeneous catalytic systems have recently been reported.<sup>60-62</sup> Furthermore, examples of catalytic hydrogenation of isocyanides are rare.<sup>63-64</sup> The catalytic hydrogenation of nitriles and isocyanides were performed under identical conditions to those of nitroarene hydrogenation reactions. At a 0.5 mol % Co-loading, Zr<sub>12</sub>-TPDC-Co efficiently reduced a range of nitriles including substrates bearing bromo- and amino-functionalities to afford corresponding benzylamines in quantitative yields (entries 1-4, Table 3). Pure benzylamine products were isolated in 94-100% yields after simple filtration followed by removal of the volatiles in vacuo. The MOF recovered from the hydrogenation of benzonitrile remained crystalline, as shown by PXRD (Figure 3b), and the leaching of Co and Zr into the supernatant was 0.2% and 0.03%, respectively. Zr<sub>12</sub>-TPDC-Co could be recovered and reused at least 7 times for the hydrogenation of benzonitrile to afford pure benzylamine without any loss of catalytic activity (Figure 6).

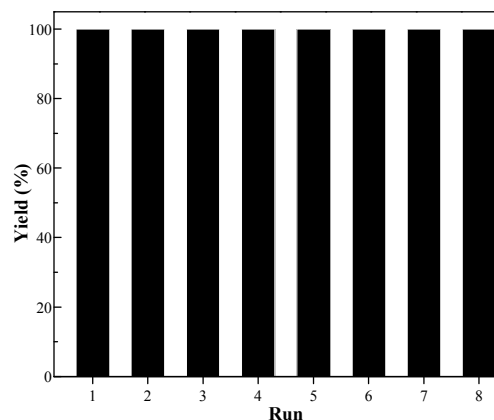
Similarly, isocyanides were also efficiently reduced to *N*-methylamines by Zr<sub>12</sub>-TPDC-Co in toluene at 110 °C under 40 bar H<sub>2</sub>. At a 0.5-2.0 mol % Co loading, benzyl isocyanide, 2-naphthyl isocyanide, cyclohexyl isocyanide, and  $\alpha$ -methylbenzyl isocyanide were hydrogenated in 100% conversion to afford *N*-benzylmethylamine, *N*-methyl-*N*-2-naphthylamine, *N*-methyl-cyclohexylamine and *N*-methyl- $\alpha$ -methylbenzylamine, respectively. Pure secondary amines were isolated in 82-96% yields (entries 5-8, Table 3). The leaching of Co and Zr into the supernatant after hydrogenation of 2-naphthyl isocyanide was determined to be 0.2% and 0.08%, respectively.

**Table 3.** Zr<sub>12</sub>-TPDC-Co Catalyzed Hydrogenation of Nitrile and Isocyanide Compounds.<sup>a</sup>

Entry	Substrate	Product	Mol % Co	Yield % <sup>b</sup>
1			0.5	100
2			0.5	100
3			0.5	100 (94)

4			0.5	100 (98)
5			2	100 (93)
6			1.0	100 (96)
7			0.5	92
8			0.5	82

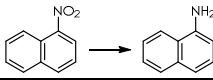
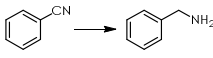
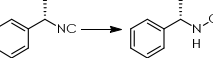
<sup>a</sup>Reaction conditions: 0.50 mg of Zr<sub>12</sub>-TPDC-Co for nitrile substrates, 2.0 mg of Zr<sub>12</sub>-TPDC-Co for isocyanide substrates, nitrile or isocyanide, toluene, 40 bar H<sub>2</sub>, 110 °C, 42 h. <sup>b</sup>Yield was determined by <sup>1</sup>H NMR with mesitylene as the internal standard. Isolated yields are in parentheses.



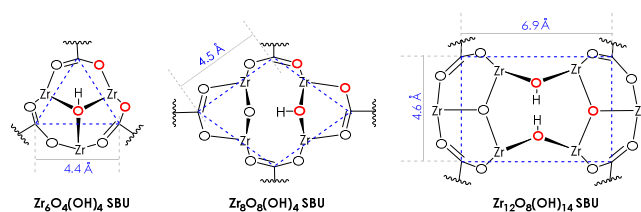
**Figure 6.** Plots of yields (%) of benzylamine at different runs in the recycle experiments of Zr<sub>12</sub>-TPDC-Co for the hydrogenation of benzonitrile. The Co-loadings were 1.0 mol %.

**Catalytic Activity Comparison of Zr<sub>12</sub>-TPDC-Co, Zr<sub>6</sub>-TPDC-Co, and Zr<sub>8</sub>-MTBC-Co Systems.** To investigate the electronic and steric differences of the Co centers in Zr<sub>12</sub>-TPDC-Co and those in previously reported Zr<sub>6</sub>-TPDC-Co and Zr<sub>8</sub>-MTBC-Co, we set up catalytic hydrogenation of selected substrates for all three types of reactions under identical conditions. For hydrogenation of 1-nitronaphthalene (entry 1, Table 4), Zr<sub>12</sub>-TPDC-Co gave complete conversion to 1-aminonaphthalene, while Zr<sub>6</sub>-TPDC-Co and Zr<sub>8</sub>-MTBC-Co were completely inactive for this substrate. Nano-sized Zr<sub>6</sub>-TPDC-Co of ~160 nm in diameter was also inactive for any of the hydrogenation reactions (Figure S17, Table S7, SI), ruling out the major contribution of MOF crystallite sizes to the catalytic activity differences among the three systems.<sup>65</sup> The drastically different activities of the three Co@SBU catalysts can be explained by the steric difference among the three SBUs. The Co-binding site in Zr<sub>12</sub>-SBU is featured by a sterically open 4.6 Å × 6.9 Å rectangle space, while the Zr<sub>6</sub>-SBU site is an equilateral triangle with edge length of 4.4 Å and the Zr<sub>8</sub>-SBU site is a rhombus with an edge length of 4.5 Å (Figure 7 and Figure S12, SI).

**Table 4.** Hydrogenation of Nitroarene, Nitrile and Isocyanide Compounds with Different SBU Supported Co-catalysts.

Entry	Reactions	Zr <sub>6</sub> -TPDC-CoH	Zr <sub>8</sub> -MTBC-CoH	Zr <sub>12</sub> -TPDC-CoH
1 <sup>a</sup>		0 %	0 %	100 %
2 <sup>b</sup>		0 %	4 %	100 %
3 <sup>c</sup>		0 %	7 %	82 %

<sup>a</sup>Reaction conditions: 0.5 mol% of Zr-MOF-Co catalyst, 1-nitronaphthalene (69 mg, 0.4 mmol), toluene, 40 bar H<sub>2</sub>, 110 °C, 42 h. <sup>b</sup>Reaction conditions: 0.5 mol% of Zr-MOF-Co catalyst, benzonitrile (42 μL, 0.4 mmol), toluene, 40 bar H<sub>2</sub>, 110 °C, 42 h. <sup>c</sup>Reaction conditions: 0.5 mol% of Zr-MOF-Co catalyst, (S)-(-)-α-methylbenzyl isocyanide (54 μL, 0.4 mmol), toluene, 40 bar H<sub>2</sub>, 110 °C, 42 h.

**Figure 7.** Comparison of the electronic and steric properties of Co binding sites in Zr<sub>6</sub>, Zr<sub>8</sub>, and Zr<sub>12</sub> SBUs. The oxygen atoms highlighted in red are involved in cobalt binding after lithiation and metalation.

For hydrogenation of benzonitrile, Zr<sub>12</sub>-TPDC-Co afforded benzylamine in a quantitative yield while Zr<sub>6</sub>-TPDC-Co and Zr<sub>8</sub>-MTBC-Co produced benzylamine in 0% and 4% yields, respectively. We believe that the higher activity of Zr<sub>12</sub>-TPDC-Co in nitrile reduction mainly stems from the dianionic nature of the binding site, leading to a more electron-rich Co center which should facilitate the migratory insertion of hydride to the nitrile triple bond. Zr<sub>12</sub>-TPDC-Co is also significantly more active than Zr<sub>6</sub>-TPDC-Co and Zr<sub>8</sub>-MTBC-Co in isocyanide hydrogenation. For example, Zr<sub>12</sub>-TPDC-Co catalyzed the hydrogenation of sterically hindered (S)-(-)-α-methylbenzyl isocyanide to afford the secondary amine product in 82% yield (entry 3, Table 4), while Zr<sub>6</sub>-TPDC-Co was totally inactive and Zr<sub>8</sub>-MTBC-Co gave only 7% of the hydrogenation product. The electron-rich nature of and more sterically open environment around the [(μ<sub>2</sub>-O)<sub>2</sub>(μ<sub>3</sub>-O)CoH]<sup>-</sup> active sites are likely responsible for the much higher activity of the Zr<sub>12</sub>-TPDC-Co catalyst.

## Conclusion

We have synthesized the first Zr MOF based on novel Zr<sub>12</sub>(μ<sub>3</sub>-O)<sub>8</sub>(μ<sub>3</sub>-OH)<sub>8</sub>(μ<sub>2</sub>-OH)<sub>6</sub> nodes. The Zr<sub>12</sub> SBUs provide a unique ligand environment for Co(II) centers to afford a

highly effective single-site solid catalyst for the hydrogenation of nitroarenes, nitriles, and isocyanides. The monomeric pathway was proposed for the nitroarene hydrogenation reaction by comparing hydrogenation reactivities of all possible intermediates. The Zr<sub>12</sub>-TPDC-Co catalyst represents the first base-metal catalyst for the hydrogenation of isocyanides to N-methylamines. The straightforward SBU functionalization and the exceptional catalytic activity of Zr<sub>12</sub>-TPDC-Co indicates that MOF nodes can provide an unprecedented ligand platform to design recyclable and reusable earth-abundant metal catalysts for sustainable synthesis of fine and commodity chemicals.

## ASSOCIATED CONTENT

**Supporting Information.** Synthesis and characterization of Zr<sub>12</sub>-TPDC, Zr<sub>12</sub>-TPDC-CoCl, Zr<sub>12</sub>-TPDC-Co; Structural model of Zr<sub>12</sub>-TPDC and Co coordination in Zr<sub>12</sub>-TPDC-CoCl and Zr<sub>12</sub>-TPDC-Co; Details for X-ray absorption spectroscopic analysis, crystallographic data; Space-filling models of Zr<sub>12</sub>-TPDC-Co; Zr<sub>6</sub>-TPDC-Co, and Zr<sub>8</sub>-MTBC-Co; Reaction procedures and product characterizations for catalytic hydrogenation of nitroarenes, nitriles, and isocyanides; This material is available free of charge via the Internet at <http://pubs.acs.org>. Crystallographic data of Zr<sub>12</sub>-Formate (CCDC 1524012) can be obtained free of charge from The Cambridge Crystallographic Data Centre via [www.ccdc.cam.ac.uk/data\\_request/cif](http://www.ccdc.cam.ac.uk/data_request/cif).

## AUTHOR INFORMATION

### Corresponding Author

\*wenbinlin@uchicago.edu

### Author Contributions

<sup>†</sup>These authors contributed equally.

### Notes

The authors declare no competing financial interest.

## ACKNOWLEDGMENT

This work was supported by NSF (CHE-1464941). We thank Guangxu Lan, Marek Piechowicz, and Daniel Micheroni for experimental help. XAS analysis was performed at Beamline 10-BM, Advanced Photon Source (APS), Argonne National Laboratory (ANL). Single crystal X-ray diffraction studies were performed at ChemMatCARS, APS, ANL. ChemMatCARS is principally supported by the Divisions of Chemistry (CHE) and Materials Research (DMR), NSF, under grant number NSF/CHE-1346572. Use of the Advanced Photon Source, an Office of Science User Facility operated for the U.S. DOE Office of Science by ANL, was supported by the U.S. DOE under Contract No. DE-AC02-06CH11357.

## References

- Sawano, T.; Ji, P.; McIsaac, A. R.; Lin, Z.; Abney, C. W.; Lin, W., *Chem. Sci.* **2015**, *6* (12), 7163-7168.
- Ma, L.; Abney, C.; Lin, W., *Chem. Soc. Rev.* **2009**, *38* (5), 1248-1256.



3. Lee, J.; Farha, O. K.; Roberts, J.; Scheidt, K. A.; Nguyen, S. T.; Hupp, J. T., *Chem. Soc. Rev.* **2009**, *38* (5), 1450-1459.
4. Tanabe, K. K.; Cohen, S. M., *Chem. Soc. Rev.* **2011**, *40* (2), 498-519.
5. Manna, K.; Zhang, T.; Carboni, M.; Abney, C. W.; Lin, W., *J. Am. Chem. Soc.* **2014**, *136* (38), 13182-13185.
6. Manna, K.; Zhang, T.; Greene, F. X.; Lin, W., *J. Am. Chem. Soc.* **2015**, *137* (7), 2665-2673.
7. Srirambalaji, R.; Hong, S.; Natarajan, R.; Yoon, M.; Hota, R.; Kim, Y.; Ho Ko, Y.; Kim, K., *Chem. commun.* **2012**, *48* (95), 11650-11652.
8. Hwang, Y. K.; Hong, D.-Y.; Chang, J.-S.; Jhung, S. H.; Seo, Y.-K.; Kim, J.; Vimont, A.; Daturi, M.; Serre, C.; Férey, G., *Angew. Chem. Int. Ed.* **2008**, *47* (22), 4144-4148.
9. Della Rocca, J.; Liu, D.; Lin, W., *Acc. Chem. Res.* **2011**, *44* (10), 957-968.
10. Horcajada, P.; Serre, C.; Vallet-Regí, M.; Sebban, M.; Taulelle, F.; Férey, G., *Angew. Chem. Int. Ed.* **2006**, *45* (36), 5974-5978.
11. Horcajada, P.; Gref, R.; Baati, T.; Allan, P. K.; Maurin, G.; Couvreur, P.; Férey, G.; Morris, R. E.; Serre, C., *Chem. Rev.* **2011**, *112* (2), 1232-1268.
12. Li, B.; Wen, H. M.; Cui, Y.; Zhou, W.; Qian, G.; Chen, B., *Adv. Mater.* **2016**, *28* (40), 8819-8860.
13. Murray, L. J.; Dincă, M.; Long, J. R., *Chem. Soc. Rev.* **2009**, *38* (5), 1294-1314.
14. Rowsell, J. L.; Yaghi, O. M., *Angew. Chem. Int. Ed.* **2005**, *44* (30), 4670-4679.
15. Kitagawa, S.; Uemura, K., *Chem. Soc. Rev.* **2005**, *34* (2), 109-119.
16. Li, J.-R.; Sculley, J.; Zhou, H.-C., *Chem. Rev.* **2011**, *112* (2), 869-932.
17. Rosi, N. L.; Eckert, J.; Eddaoudi, M.; Vodak, D. T.; Kim, J.; O'Keeffe, M.; Yaghi, O. M., *Science* **2003**, *300* (5622), 1127-1129.
18. Xiang, S.-C.; Zhang, Z.; Zhao, C.-G.; Hong, K.; Zhao, X.; Ding, D.-R.; Xie, M.-H.; Wu, C.-D.; Das, M. C.; Gill, R.; Thomas, K. M.; Chen, B., *Nat. Commun.* **2011**, *2*, 204.
19. Suh, M. P.; Park, H. J.; Prasad, T. K.; Lim, D.-W., *Chem. Rev.* **2011**, *112* (2), 782-835.
20. Eddaoudi, M.; Kim, J.; Rosi, N.; Vodak, D.; Wachter, J.; O'Keeffe, M.; Yaghi, O. M., *Science* **2002**, *295* (5554), 469-472.
21. Kreno, L. E.; Leong, K.; Farha, O. K.; Allendorf, M.; Van Duyne, R. P.; Hupp, J. T., *Chem. Rev.* **2011**, *112* (2), 1105-1125.
22. Allendorf, M. D.; Houk, R. J. T.; Andruszkiewicz, L.; Talin, A. A.; Pikarsky, J.; Choudhury, A.; Gall, K. A.; Hesketh, P. J., *J. Am. Chem. Soc.* **2008**, *130* (44), 14404-14405.
23. Lan, A.; Li, K.; Wu, H.; Olson, D. H.; Emge, T. J.; Ki, W.; Hong, M.; Li, J., *Angew. Chem. Int. Ed.* **2009**, *48* (13), 2334-2338.
24. Lin, W.; Long, J. R., *Inorg. Chem.* **2016**, *55* (15), 7189.
25. Kent, C. A.; Liu, D.; Ma, L.; Papanikolas, J. M.; Meyer, T. J.; Lin, W., *J. Am. Chem. Soc.* **2011**, *133* (33), 12940-12943.
26. Sun, L.; Campbell, M. G.; Dincă, M., *Angew. Chem. Int. Ed.* **2016**, *55* (11), 3566-3579.
27. Silva, C. G.; Corma, A.; Garcia, H., *J. Mater. Chem.* **2010**, *20* (16), 3141-3156.
28. Ji, P.; Sawano, T.; Lin, Z.; Urban, A.; Boures, D.; Lin, W., *J. Am. Chem. Soc.* **2016**, *138* (45), 14860-14863.
29. Hendon, C. H.; Tiana, D.; Fontecave, M.; Sanchez, C. m.; D'arras, L.; Sassoie, C.; Rozes, L.; Mellot-Draznieks, C.; Walsh, A., *J. Am. Chem. Soc.* **2013**, *135* (30), 10942-10945.
30. Schoedel, A.; Li, M.; Li, D.; O'Keeffe, M.; Yaghi, O. M., *Chem. Rev.* **2016**, *116* (19), 12466-12535.
31. Fukino, T.; Joo, H.; Hisada, Y.; Obana, M.; Yamagishi, H.; Hikima, T.; Takata, M.; Fujita, N.; Aida, T., *Science* **2014**, *344* (6183), 499-504.
32. Zhang, W.-X.; Liao, P.-Q.; Lin, R.-B.; Wei, Y.-S.; Zeng, M.-H.; Chen, X.-M., *Coord. Chem. Rev.* **2015**, *293*, 263-278.
33. Bai, Y.; Dou, Y.; Xie, L.-H.; Rutledge, W.; Li, J.-R.; Zhou, H.-C., *Chem. Soc. Rev.* **2016**, *45* (8), 2327-2367.
34. Devic, T.; Serre, C., *Chem. Soc. Rev.* **2014**, *43* (16), 6097-6115.
35. Mouchaham, G.; Cooper, L.; Guillou, N.; Martineau, C.; Elkaim, E.; Bourrelly, S.; Llewellyn, P. L.; Allain, C.; Clavier, G.; Serre, C., *Angew. Chem. Int. Ed.* **2015**, *127* (45), 13495-13499.
36. Guillerm, V.; Ragon, F.; Dan - Hardi, M.; Devic, T.; Vishnuvarthan, M.; Campo, B.; Vimont, A.; Clet, G.; Yang, Q.; Maurin, G., *Angew. Chem. Int. Ed.* **2012**, *51* (37), 9267-9271.
37. Cavka, J. H.; Jakobsen, S.; Olsbye, U.; Guillou, N.; Lamberti, C.; Bordiga, S.; Lillerud, K. P., *J. Am. Chem. Soc.* **2008**, *130* (42), 13850-13851.
38. Furukawa, H.; Gándara, F.; Zhang, Y.-B.; Jiang, J.; Queen, W. L.; Hudson, M. R.; Yaghi, O. M., *J. Am. Chem. Soc.* **2014**, *136* (11), 4369-4381.
39. Ji, P.; Manna, K.; Lin, Z.; Urban, A.; Greene, F. X.; Lan, G.; Lin, W., *J. Am. Chem. Soc.* **2016**, *138* (37), 12234-12242.
40. Zhang, X.; Zhang, X.; Johnson, J. A.; Chen, Y.-S.; Zhang, J., *J. Am. Chem. Soc.* **2016**, *138* (27), 8380-8383.
41. Piszczek, P.; Radtke, A.; Wojtczak, A.; Muzioł, T.; Chojnacki, J., *Polyhedron* **2009**, *28* (2), 279-285.
42. Manna, K.; Ji, P.; Lin, Z.; Greene, F. X.; Urban, A.; Thacker, N. C.; Lin, W., *Nat. Commun.* **2016**, *7*, 12610.
43. Ono, N., *The nitro group in organic synthesis*. John Wiley & Sons: 2003; Vol. 9.
44. Sheldon, R. A.; Van Bekkum, H., *Fine chemicals through heterogeneous catalysis*. John Wiley & Sons: Weinheim, Germany, 2008.
45. Blaser, H.-U.; Steiner, H.; Studer, M., *ChemCatChem* **2009**, *1* (2), 210-221.
46. Li, J.; Shi, X.-Y.; Bi, Y.-Y.; Wei, J.-F.; Chen, Z.-G., *ACS Catal.* **2011**, *1* (6), 657-664.
47. Corma, A.; Serna, P., *Science* **2006**, *313* (5785), 332-334.
48. Westerhaus, F. A.; Jagadeesh, R. V.; Wienhöfer, G.; Pohl, M.-M.; Radnik, J.; Surkus, A.-E.; Rabeah, J.; Junge, K.; Junge, H.; Nielsen, M.; Brückner, A.; Beller, M., *Nat Chem* **2013**, *5* (6), 537-543.
49. Wienhöfer, G.; Sorribes, I.; Boddien, A.; Westerhaus, F.; Junge, K.; Junge, H.; Llusar, R.; Beller, M., *J. Am. Chem. Soc.* **2011**, *133* (32), 12875-12879.
50. Jagadeesh, R. V.; Surkus, A.-E.; Junge, H.; Pohl, M.-M.; Radnik, J.; Rabeah, J.; Huan, H.; Schünemann, V.; Brückner, A.; Beller, M., *Science* **2013**, *342* (6162), 1073-1076.
51. Schwob, T.; Kempe, R., *Angew. Chem. Int. Ed.* **2016**, *55* (48), 15175-15179.
52. Wienhöfer, G.; Sorribes, I.; Boddien, A.; Westerhaus, F.; Junge, K.; Junge, H.; Llusar, R.; Beller, M., *J. Am. Chem. Soc.* **2011**, *133* (32), 12875-12879.
53. Seyden-Penne, J., *Reductions by the alumino-and borohydrides in organic synthesis*. John Wiley & Sons: Weinheim, Germany, 1997.
54. Laval, S.; Dayoub, W.; Favre-Reguillon, A.; Berthod, M.; Demonchaux, P.; Mignani, G.; Lemaire, M., *Tetrahedron Lett.* **2009**, *50* (50), 7005-7007.
55. Bornschein, C.; Werkmeister, S.; Junge, K.; Beller, M., *New J. Chem* **2013**, *37* (7), 2061-2065.

- 1 56. Reguillo, R.; Grellier, M.; Vautravers, N.; Vendier, L.; Sabo-  
2 Etienne, S., *J. Am. Chem. Soc* **2010**, *132* (23), 7854-7855.  
3 57. Srimani, D.; Feller, M.; Ben-David, Y.; Milstein, D., *Chem.*  
4 *commun.* **2012**, *48* (97), 11853-11855.  
5 58. Enthaler, S.; Addis, D.; Junge, K.; Erre, G.; Beller, M., *Chem.*  
6 *Eur. J.* **2008**, *14* (31), 9491-9494.  
7 59. Li, T.; Bergner, I.; Haque, F. N.; Zimmer-De Iuliis, M.; Song,  
8 D.; Morris, R. H., *Organometallics* **2007**, *26* (24), 5940-5949.  
9 60. Mukherjee, A.; Srimani, D.; Chakraborty, S.; Ben-David, Y.;  
10 Milstein, D., *J. Am. Chem. Soc* **2015**, *137* (28), 8888-8891.  
11 61. Chen, F.; Topf, C.; Radnik, J. r.; Kreyenschulte, C.; Lund, H.;  
12 Schneider, M.; Surkus, A.-E.; He, L.; Junge, K.; Beller, M., *J. Am.*  
13 *Chem. Soc* **2016**, *138* (28), 8781-8788.  
14 62. Bornschein, C.; Werkmeister, S.; Wendt, B.; Jiao, H.;  
15 Alberico, E.; Baumann, W.; Junge, H.; Junge, K.; Beller, M., *Nat.*  
16 *Commun* **2014**, *5*, 4111.  
17 63. Carpenter, A. E.; Rheingold, A. L.; Figueroa, J. S.,  
18 *Organometallics* **2016**, *35* (14), 2309-2318.  
19 64. Band, E.; Pretzer, W.; Thomas, M.; Muetterties, E., *J. Am.*  
20 *Chem. Soc* **1977**, *99* (22), 7380-7381.  
21 65. Hermannsdörfer, J.; Friedrich, M.; Kempe, R., *Chem. Eur. J.*  
22 **2013**, *19* (41), 13652-13657.

23  
24 **For Table of Contents Only:**

